

RESEARCH

Open Access



# Cytotoxicity and reactive oxygen species production induced by different co-monomer eluted from nanohybrid dental composites

En-Shi Jiang<sup>1,2</sup>, Wonjoon Moon<sup>1,3,4</sup>, Bum-Soon Lim<sup>1</sup>, Juhea Chang<sup>5\*†</sup> and Shin Hye Chung<sup>1\*†</sup>

## Abstract

**Background** Safety issues for dental restorative composites are critical to material selection, but, limited information is available to dental practitioners. This study aimed to compare the chemical and biological characteristics of three nanohybrid dental composites by assessing filler particle analysis, monomer degree of conversion (DC), the composition of eluates, and cytotoxicity and reactive oxygen species (ROS) production in fibroblasts.

**Methods** Three nanohybrid composites (TN, Tetric N-Ceram; CX, Ceram X Sphere Tec One; and DN, DenFil NX) were used. The size distribution and morphology of the filler particles were analysed using scanning electron microscopy ( $n = 5$ ). The DC was measured via micro-Raman spectroscopy ( $n = 5$ ). For the component analysis, methanol eluates from the light-polymerised composites were evaluated by gas chromatography/mass spectrometry ( $n = 3$ ). The eluates were prepared from the polymerised composites after 24 h in a cell culture medium. A live/dead assay ( $n = 9$ ) and Water-Soluble Tetrazolium-1 assay ( $n = 9$ ) were performed and compared with negative and positive controls. The ROS in composites were compared with NC. Statistical significance in differences was assessed using a t-test and ANOVA ( $\alpha = 0.05$ ).

**Results** Morphological variations in different-sized fillers were observed in the composites. The DC values were not significantly different among the composites. The amounts of 2-hydroxyethyl methacrylate (HEMA) were higher in TN than DN ( $p = 0.0022$ ) and triethylene glycol dimethacrylate (TEGDMA) in CX was higher than in others ( $p < 0.0001$ ). The lowest cell viability was shown in CX ( $p < 0.0001$ ) and the highest ROS formation was detected in TN ( $p < 0.0001$ ).

**Conclusions** Three nanohybrid dental composites exhibited various compositions of filler sizes and resin components, resulting in different levels of cytotoxicity and ROS production. Chemical compositions of dental composites can be considered with their biological impact on safety issues in the intraoral use of dental restorative composites. CX with the highest TEGDMA showed the highest cytotoxicity induced by ROS accumulation. DN with lower TEGDMA and HEMA presented the highest cell viability.

**Keywords** Nanohybrid, Dental composites, Eluates, Cytotoxicity, Reactive oxygen species, Gas chromatography/mass spectrometry

<sup>†</sup>Juhea Chang, Shin Hye Chung equally contributed to this work as corresponding authors

\*Correspondence:  
Juhea Chang  
juhchang@snu.ac.kr  
Shin Hye Chung  
den533@snu.ac.kr

Full list of author information is available at the end of the article



© The Author(s) 2023. **Open Access** This article is licensed under a Creative Commons Attribution 4.0 International License, which permits use, sharing, adaptation, distribution and reproduction in any medium or format, as long as you give appropriate credit to the original author(s) and the source, provide a link to the Creative Commons licence, and indicate if changes were made. The images or other third party material in this article are included in the article's Creative Commons licence, unless indicated otherwise in a credit line to the material. If material is not included in the article's Creative Commons licence and your intended use is not permitted by statutory regulation or exceeds the permitted use, you will need to obtain permission directly from the copyright holder. To view a copy of this licence, visit <http://creativecommons.org/licenses/by/4.0/>. The Creative Commons Public Domain Dedication waiver (<http://creativecommons.org/publicdomain/zero/1.0/>) applies to the data made available in this article, unless otherwise stated in a credit line to the data.

## Background

The wide-ranged applications of resin-based composites in restorative dentistry facilitated the improvement of the mechanical and aesthetic features as well as clinical performance. To enhance the material properties, various technologies have been introduced, mainly those dealing with changes in filler components and monomer-matrix formulation [1–4]. Among restorative composite resins with various filler distributions, nanohybrid composites incorporate both nano-ranged sizes of inorganic fillers (0.005–0.01  $\mu\text{m}$ ) and microsized fillers (0.01–0.04  $\mu\text{m}$ ) [5]. The nano-sized fillers, are smaller than the visible light wavelengths and occupy the spaces between larger particles. Additional filler loading by submicron-sized particles led to improved surface qualities such as superior polish and gloss retention compared to conventional micro-hybrid composites [6, 7]. However, small sizes of filler particles increase the surface area-to-volume ratios of the fillers, which may make the polymerised structures prone to water uptake and induce interfacial degradation of the resin matrix and filler particles [8]. In addition, water absorption and moisture permeation into the pores within the incompletely regarding the monomers and additives released from resin-based composites leaching into the oral environment in diverse polymerizing conditions [11–13]. Cell death caused by DNA double-strand breakage, alveolar bone resorption by increased inflammatory cytokine activity, the inflammatory reaction by increased COX-2 enzyme, and acute systemic toxicity are significant concerns of leached components [14–17]. Bisphenol-A (BPA) is a well-known endocrine disruptor that can be present as an impurity or degradation product of BPA-based monomers [18]. Co-monomers of low molecular weight, such as triethylene glycol dimethacrylate (TEGDMA) and 2-hydroxyethyl methacrylate (HEMA), are more mobile and absorbent and readily leach into the immersion medium relative to basic monomers with high molecular weights, such as bisphenol A glycidyl methacrylate (Bis-GMA), bisphenol A ethoxy-dimethacrylate (Bis-EMA), and urethane dimethacrylate (UDMA) [11]. Exposure to TEGDMA, HEMA, or UDMA can produce reactive oxygen species (ROS) leading to cell damage [19, 20]. Further, the elevation of exposure levels can detrimentally induce DNA damage and cell death [21–23].

Considering the large variety of compositions in light-polymerised composites and their diverse usage in restorative dentistry, the potential risks of resin components leaching out into the oral cavity can be a significant concern to patients and practitioners. Therefore, it is meaningful that the biocompatibility of polymerised resins is assessed at the level of individual eluates both in quantitative and qualitative manners. Gas chromatography/

mass spectrometry (GC/MS) has been used to identify additives, smaller monomers, comonomers and other volatile compounds, and decomposition and fragmentation products [24]. A strong correlation between the amount of eluates and cell viability was largely manifested using various cell lines and different test methods [22, 25–29]. Further, components released from polymerised composites can affect cellular signalling networks by generating ROS, in the same pattern as detected with cytotoxic effects [26]. Moreover, the crosslinking structures of matrix monomers and dispersed inorganic fillers can have mutual impacts on the reachability of unbound monomers, thus the filler contents are an interesting topic for investigating the toxicity of composite materials. However, limited information is available to dental practitioners when selecting the material considering safety issues in relation to leaching components of nanohybrid composites [13].

This study aimed to compare the chemical and biological characteristics of three nanohybrid dental composites by assessing filler particle analysis, monomer degree of conversion (DC), the composition of elutes, and cytotoxicity and ROS production in fibroblasts. The null hypothesis was that the components eluted from the three tested nanohybrid dental composites would show no differences in cytotoxicity or ROS production.

## Materials and methods

### Overview

Three nanohybrid composite resins (Tetric N-Ceram, TN; Ceram X Sphere Tec One, CX; and DenFil NX, DN) were used in the study (Table 1). The variables of filler contents, DC, and eluate compositions were determined using scanning electron microscopy (SEM) analysis, micro Raman spectroscopy, and GC/MS. Live/dead and Water-Soluble Tetrazolium-1 assays were performed for cytotoxicity evaluation and real-time ROS production was assessed in fibroblasts (Fig. 1).

### Filler particle analysis

#### Filler particle preparation

For the filler particle characterization, the resin matrix of the composites (TN, CX, and DN) was dissolved and discarded to separate the fillers. A total of 300 mg of unpolymerised composites were placed in 10 mL amber glass vials, then immersed in 6 mL of acetone (99.5%, Sigma-Aldrich St. Louis, MO, USA) chloroform (99.8%, Sigma-Aldrich) and absolute ethanol (Sigma-Aldrich) successively and held for 24 h per each. While holding, the samples were centrifuged three times at 1,200 rpm for 6 min, and the supernatants were discarded. The remaining precipitation was dried overnight at 37 °C and sputter-coated for SEM observation.

**Table 1** Materials used in the study

Group	Type	Matrix composition	Filler composition	Filler degree (vol%, wt%)	Manufacturer (Lot No.)
TN	Nanohybrid	Bis-GMA, UDMA, Bis-EMA, TEGDMA	Barium aluminium glass (0.4 µm, 0.7 µm), Ytterbium trifluoride (0.2 µm), Mixed oxide (0.16 µm), Prepolymer	55–57, 76	Ivoclar Vivadent, Lichtenstein (Y50557)
CX	Nanohybrid ceramic	Bis-EMA, TEGDMA	The Sphere TEC fillers (15 µm), Nonagglomerated barium glass fillers (0.6 µm), Ytterbium fluoride (0.6 µm), Methacrylic polysiloxane, nanoparticles	59–61, 77–79	Dentsply Sirona, USA (2,009,000,471)
DN	Nanohybrid	Bis-GMA, UDMA, TEGDMA	Barium aluminosilicate (< 1 µm), Fumed silica (0.04 µm)	76–78, 81	Vericom, Korea (NX1601A2)

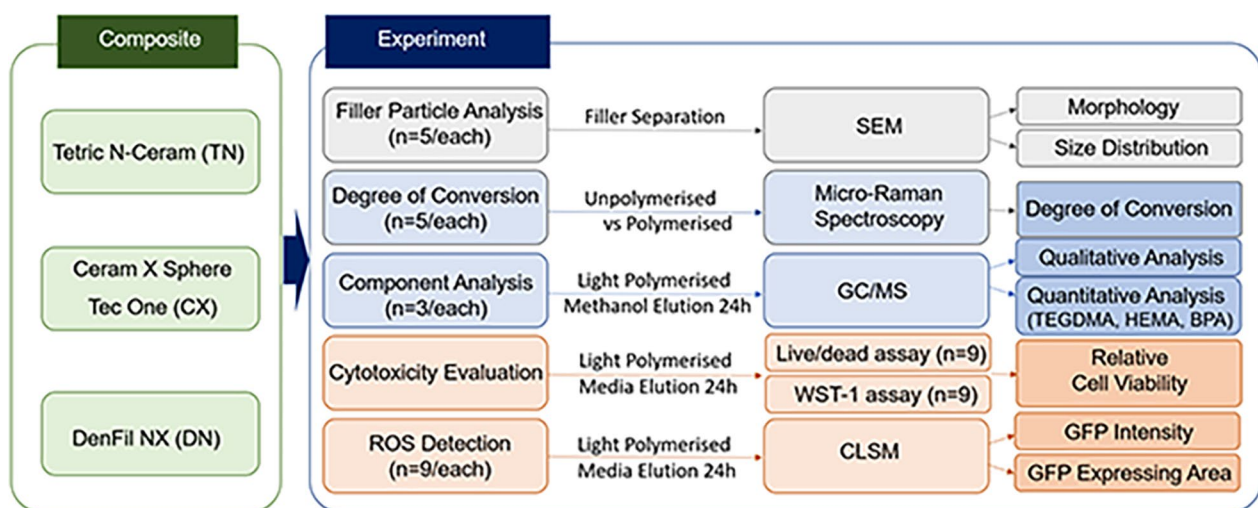


**Fig. 1** Experimental flow diagram

**SEM observation**

The morphology and the size distribution of filler particles were observed under SEM (S-4700, FE-SEM, Hitachi, Tokyo, Japan) ( $n=5$ ). SEM images were taken at 10 kV, 0.1 nA, and a working distance of 10 mm at magnifications of 1,000, 5,000, and 30,000. The size and number of submicron-sized (smaller than 1 µm) were determined from 1,000 random particles at a magnification of 30,000 ( $n=5$ ). The spherical-shaped fillers were assessed from 100 random particles ( $n=5$ ) at 5,000 × and 30,000 ×. ImageJ software (ver. 1.53, National Institutes of Health, Bethesda, MD, USA) was used for the image analysis [31, 32].

**Degree of conversion measurement**

**Specimen preparation**

The composites (TN, CX, and DN) were prepared into disc-shaped specimens (13 mm diameter and 1 mm thickness) in a Teflon mould. Both top and bottom

surfaces were cured for 40 s using a light-emitting diode (LED) curing unit with a wavelength of 430 – 480 nm and an intensity of 850 – 950 mW/cm<sup>2</sup> (Elipar DeepCure-S LED Curing Light, 3 M ESPE, Seefeld, Germany). The top surface remained open to simulate the clinical situation of an oxygen-inhibited layer, while the bottom was covered with a glass slide.

**micro-Raman spectroscopy**

After light-polymerised, five points of each specimen ( $n=5$ ) were assessed with a 532 nm laser-equipped, micro-Raman microscope (DXR2xi, Thermo Fisher Scientific, Madison, WI, USA), showing a spectral resolution of approximately 5 cm<sup>-1</sup> and a spectral range of 2000 – 1000 cm<sup>-1</sup> at a magnification of 50. During the polymerisation, the intensity of the peak decreased with the conversion of the aliphatic double-carbon structure to form polymer chains. The following equation was used to calculate DC:

$$DC (\%) = 1 - \frac{R_{\text{Polymerised}}}{R_{\text{Unpolymerised}}} \times 100$$

where  $R$  is the ratio of peak intensity at  $1639 \text{ cm}^{-1}$  and  $1609 \text{ cm}^{-1}$  associated with the aliphatic and aromatic stretching in nanohybrid composites, respectively.

### Eluted component analysis

#### Sample preparation

To effectively achieve the maximum concentration of eluates, methanol (99.9%, Sigma-Aldrich) was used as an eluent. Three disc-shaped specimens (TN, CX, and DN) with 13 mm in diameter and 1 mm in thickness were fabricated in a Teflon mould and light-polymerised (Elipar DeepCure-S, 3M ESPE). The top surface remained open to simulate the clinical situation of an oxygen-inhibited layer, while the bottom was covered with a glass slide. The samples were immersed in methanol and eluted for 24 h at  $37^\circ\text{C}$  in brown glass vials ( $3 \text{ cm}^2/\text{mL}$ ).

#### GC/MS analysis

The eluted monomers and additives were qualitatively analysed using GC/MS ( $n=3$ ). A Trace Ultra GC Ultra gas chromatograph linked to a triple quadrupole mass spectrometer (TSQ 8000, Thermo) was used and transfused in the splitless mode. The compounds were separated using a GC column with geometry parameters of 60 m in length, 0.25 mm in diameter, and  $0.25 \mu\text{m}$  in film thickness at a stationary phase with a split ratio of 1:10 and helium flowing at a constant rate of  $1 \text{ mL}/\text{min}$ . The GC oven was heated isothermally at  $50^\circ\text{C}$  for 2 min, heated to  $280^\circ\text{C}$  ( $25^\circ\text{C}/\text{min}$ ), held for 5 min, and then cooled to  $250^\circ\text{C}$ . With an electron ionisation source temperature of  $240^\circ\text{C}$ , the mass spectrometer (MS) was set to the full scan mode, and data were recorded (mass range  $m/z$  50 – 600) at 70 eV. For qualitative analysis, the relevant compounds were identified by comparing the retention time and mass spectra with their corresponding reference standards and the National Institute of Standards and Technology (NIST) library database [30]. The limit of quantification (LOQ) was in the range of 0.1 –  $1,000 \mu\text{g}/\text{mL}$ .

For the quantitative analysis, the standard component of UDMA (Sigma-Aldrich), HEMA (Sigma-Aldrich), TEGDMA (Sigma-Aldrich), and BPA (Sigma-Aldrich) were calibrated ( $n=3$ ).

### Cytotoxicity and ROS evaluation

#### Preparation of composite eluates

For cytotoxicity evaluation and ROS detection, three disc-shaped specimens (TN, CX, and DN) with 13 mm

in diameter and 1 mm in thickness were fabricated in a Teflon mould. The top surface remained open to simulate the clinical situation of an oxygen-inhibited layer, while the bottom was covered with a glass slide. The light-polymerised (Elipar DeepCure-S, 3 M ESPE) were immersed in Dulbecco's modified Eagle medium (DMEM, Hyclone, Logan, UT, USA) for 24 h at  $37^\circ\text{C}$  in dark (ISO 10993–5:2009). After filtering with a  $0.22 \mu\text{m}$  membrane filter unit (Corning Glass Works, Corning, NY, USA), the composite eluates were used for the following analysis.

#### Cell preparation

The human gingival fibroblast cell line (HGF-1, ATCC CRL-2014) was cultured with DMEM containing 1% penicillin (Gibco, Life Technologies, Grand Island, NY, USA), 1% streptomycin (Gibco), and 10% fetal bovine serum (Gibco) at  $37^\circ\text{C}$  in a humidified chamber with 5%  $\text{CO}_2$ . The cells were seeded in a 100 mm culture dish (SPL Life Sciences, Yeosu-si, Gyeonggi-do, Korea) and evaluated after the cells reached 80% confluence.

#### Live/dead and WST-1 assays

HGF-1 cells were seeded in a 35 mm confocal dish (SPL) at a concentration of  $2 \times 10^4$  cells/mL and incubated for 24 h. After incubation, cells were washed with phosphate-buffered solution (PBS, Gibco), treated with 1 mL of prepared composite eluates, and incubated for another 24 h. The negative control (NC) was treated with DMEM and the positive control (PC) was treated with 1 mM  $\text{H}_2\text{O}_2$  (Sigma-Aldrich).

For live/dead assay, a Live/dead Viability kit (Invitrogen, Waltham, MA, USA) was used and observed under an inverted fluorescence microscope (DS-Ri2, Nikon Corporation, Tokyo, Japan) and a confocal laser microscope (LSM 700, Carl Zeiss, Thornwood, NY, USA). Live cells were observed with green fluorescence, and dead cells were observed with bright red fluorescence.

For WST-1 assay, the EZ-Cytox cell viability assay kit (DoGen Bio, Seoul, Korea) was used to determine cytotoxicity after 24 h of treatment. The optical density (OD) was determined at 450 nm using a microplate reader (AMR-100, Allsheng, Hangzhou, Zhejiang, China). Relative cell viability was calculated as the ratio of OD of experimental groups (TN, CX, and DN) to that of NC. The experiments were triplicated ( $n=9$ ).

#### Detection of ROS

HGF-1 cells were seeded in black, flat-bottom 96 well plates (Greiner Bio-One, Frickenhausen, Germany) at a density of  $1 \times 10^4$  cells/mL and incubated for 24 h.

After incubation, the medium was changed to 100  $\mu$ L of the composites eluate-containing 5  $\mu$ M CellROX green reagent (Life Technologies, Carlsbad, CA, USA) and observed at 37  $^{\circ}$ C for 16 h. Upon oxidation, the green reagent binds to DNA, and its signal is primarily localised in both the nucleus and mitochondria. To confirm the intracellular reaction, images and fluorescence intensity were recorded at 0, 4, 8, and 16 h using a multimode plate reader (Cytation 7, BioTek, Winooski, VT, USA). Green fluorescence was detected when the reagent was oxidised by ROS and then bound to DNA. The relative intensities and ROS-production areas of green fluorescent protein (GFP) were analysed by Gen5 software (ver. 1.9, Biotek). The experiments were triplicated ( $n=9$ ).

**Statistical analysis**

Statistical significance was assessed using a t-test, one-way and two-way analysis of variance (ANOVA), followed by a Bonferroni multiple comparison test. Data were analysed using GraphPad Prism (ver. 9.0.0, GraphPad Software Inc., San Diego, CA, USA).

**Results**

**Filler particle analysis**

The materials showed morphological variations of differently-sized fillers in SEM (Fig. 2). From the result of

submicron filler distribution, particles smaller than 0.1  $\mu$ m comprised 26.09% and 27.00% of the total distribution in CX and DN, while 7.63% in TN (Fig. 3). TN exhibited irregular submicron-sized fillers mixed with small spherical particles ( $0.13 \pm 0.02 \mu$ m). In CX and DN, larger spherical particles ( $12.87 \pm 6.08 \mu$ m and  $8.98 \pm 4.11 \mu$ m, respectively), were mixed with irregularly shaped fillers of submicron sizes (Table 2).

**DC measurement**

Micro-Raman spectra were obtained immediately before and after the light polymerisation (Fig. 4A). The peak intensities of  $1609 \text{ cm}^{-1}$  at  $1639 \text{ cm}^{-1}$  were associated with C=C aliphatic and aromatic stretching bonds in a polymeric matrix, respectively. The DC values in TN ( $70.61 \pm 4.27$ ), CX ( $69.13 \pm 4.46$ ), and DN ( $72.06 \pm 3.72$ ) were not significantly different ( $p = 0.05545$ , Fig. 4B).

**Qualitative and quantitative analysis of composite elutes**

Representative GC/MS chromatograms of individual substances in TN, CX, and DN were depicted (Fig. 5). HEMA was detected in both TN and DN. TEGDMA, camphorquinone (CQ), and the co-initiator, 4-dimethylaminobenzoic acid ethyl ester (DMABEE) were detected

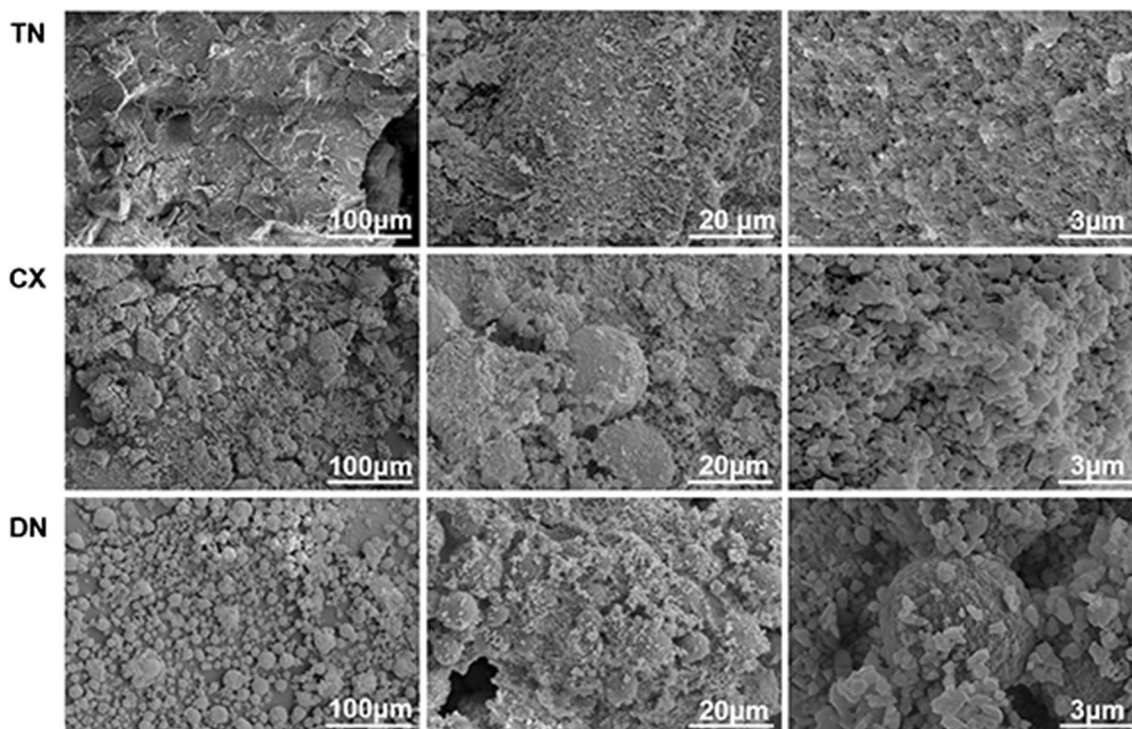


**Fig. 2** SEM images of agglomerated submicron-sized and spherical filler particles (magnification: left, 1,000  $\times$ ; centre, 5,000  $\times$ ; right, 30,000  $\times$ ). Submicron and nanofillers were aggregated to large spherical-shaped fillers (asterisk in CX and DN) that are dominant in CX and DN

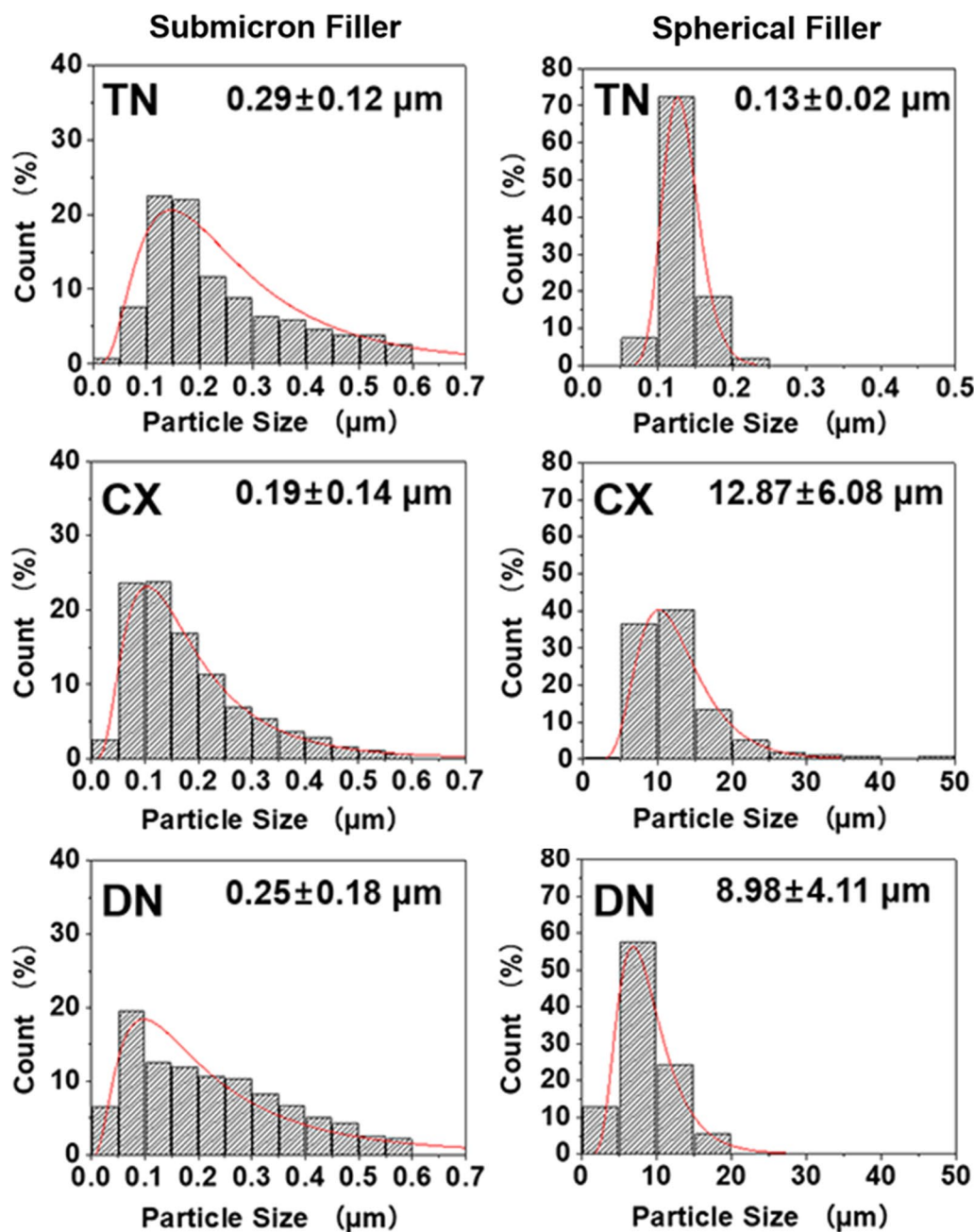


**Fig. 3** Size distributions of the filler particles. The average  $\pm$  standard deviation of each filler is shown in the graph. CX and DN had larger spherical-shaped fillers than TN

**Table 2** Mean and standard deviation of the filler particle size (μm)

	Submicron-sized	Spherical-shaped
TN	0.29 $\pm$ 0.12 <sup>a</sup>	0.13 $\pm$ 0.02 <sup>a</sup>
CX	0.19 $\pm$ 0.14 <sup>a</sup>	12.87 $\pm$ 6.08 <sup>b</sup>
DN	0.25 $\pm$ 0.18 <sup>a</sup>	8.98 $\pm$ 4.11 <sup>a</sup>
<i>p</i>	0.5027	0.0014

Different superscripts indicate significant differences in a column ( $p < 0.05$ )

in all composites. Detected components of co-monomers and other additives are listed in Table 3. Calibration curves are obtained (Fig. 6A) and the qualification analysis of standard components is presented (Fig. 6B). In UDMA, due to multiple peaks depicted in GC/MS and non linear correlation coefficient ( $R^2=0.9020$ ), the quantitative analysis was not performed with UDMA (Table 4).

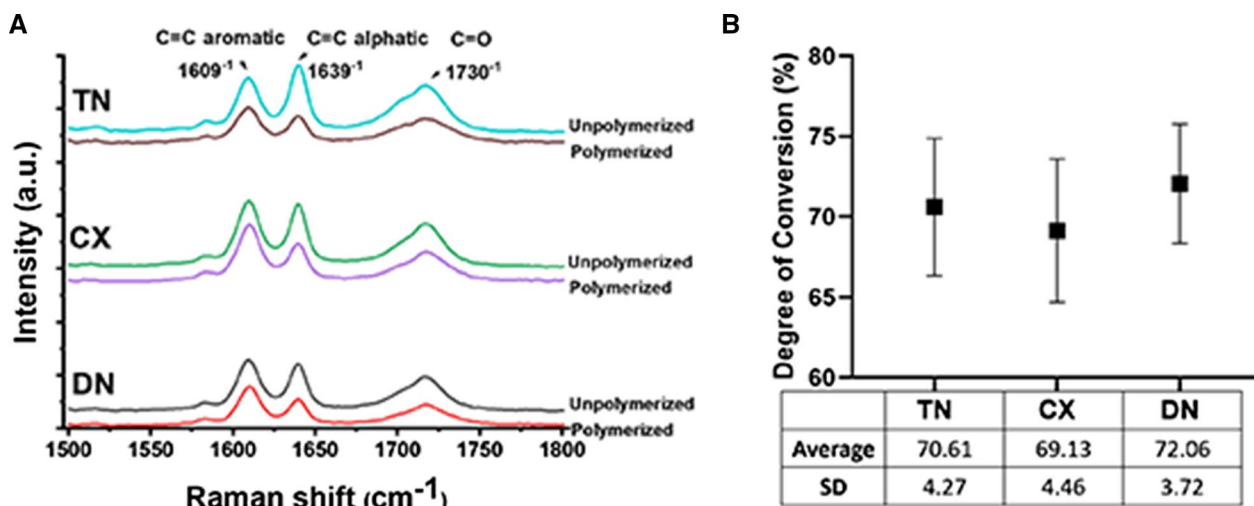


**Fig. 4** Degree of conversion. **A** Micro-Raman spectra. The intensities of 1609 cm<sup>-1</sup>, 1639 cm<sup>-1</sup>, and 1730 cm<sup>-1</sup> were used to calculate the degree of conversion. **B** The degrees of monomer conversion was not significantly different among the groups (*p* > 0.05)

The amount of HEMA in TN (259.46 ± 53.14 µg/mL) was significantly higher than that of DN (43.91 ± 3.32 µg/mL, *p* = 0.0022), and it was not detected in CX (Table 4). The amount of TEGDMA (1,081.10 ± 128.61 µg/mL) in CX was higher than those of TN and DN (23.3 ± 0.06 µg/mL, *p* < 0.0001 and 38.80 ± 3.50 µg/mL, *p* < 0.0001, respectively). BPA was not detected in any composite eluates.

**Cytotoxicity evaluation**

From the fluorescence images, TN and DN showed a slight decrease in cell density without apparent changes in cell morphology compared to NC (Fig. 7). In CX, dissimilar cell morphology with less homogeneity with shrunken cellular processes was observed.

The relative cell viability was the highest in DN (100.70 ± 6.40) with no significant difference compared to NC (Fig. 8). TN (82.10 ± 3.80) and CX (61.25 ± 3.10) showed a significant decrease in cell viability (*p* < 0.0001).

**Detection of ROS**

Fluorescent digital image correlation micrograph profiles exhibited a time-dependent increase in ROS generation (Fig. 9 and Additional file 1: Video S1). The relative intensity significantly increased in TN and CX from 8 h compared with NC (*p* < 0.0001) (Table 5 and Fig. 10A). The relative GFP expression area was calculated by relative values at zero hours (Table 6). The area in TN showed the highest ROS production followed by CX, those values were significantly higher than those in NC and DN (*p* < 0.0001) (Fig. 10B). DN showed no significant increase in ROS compared to NC until 16 h.

**Discussion**

Based on the results, three nanohybrid composites revealed different compositions of monomers and additives. HEMA and TEGDMA, representative co-monomers with low molecular weights and high mobility were eluted with different amounts in three composites, affecting the cell viability and ROS production to dissimilar levels. Therefore, our null hypothesis was rejected.

Currently, commercially available nanohybrid composites enhanced filler loading and also replaced conventional monomer-matrix formulations to maintain adequate consistency and aesthetic properties. It is common that manufacturers only indicate the total volume and weight of filler contents. Additionally, the remaining volume is occupied with resin matrix monomers and other trace additives that users are unaware of. This study focused on co-monomers of low molecular weight, which increase the polymerising effectiveness and manipulating efficiency, rather than backbone monomers of high molecular weight with elevated mechanical and chemical stabilities. Regarding the cytotoxicity of monomers released from restorative composites, the intensity of cytotoxicity of monomers was ranked as Bis-GMA > UDMA > TEGDMA > HEMA [33, 34]. However, the order of releasing tendency is known to be HEMA > TEGDMA > UDMA > BisGMA, signifying an elution capacity of small-sized monomers [11]. For methacrylate cross-linking monomers, differences exist in the magnitude of released quantities between the organic solvent and water-based solution [29]. The

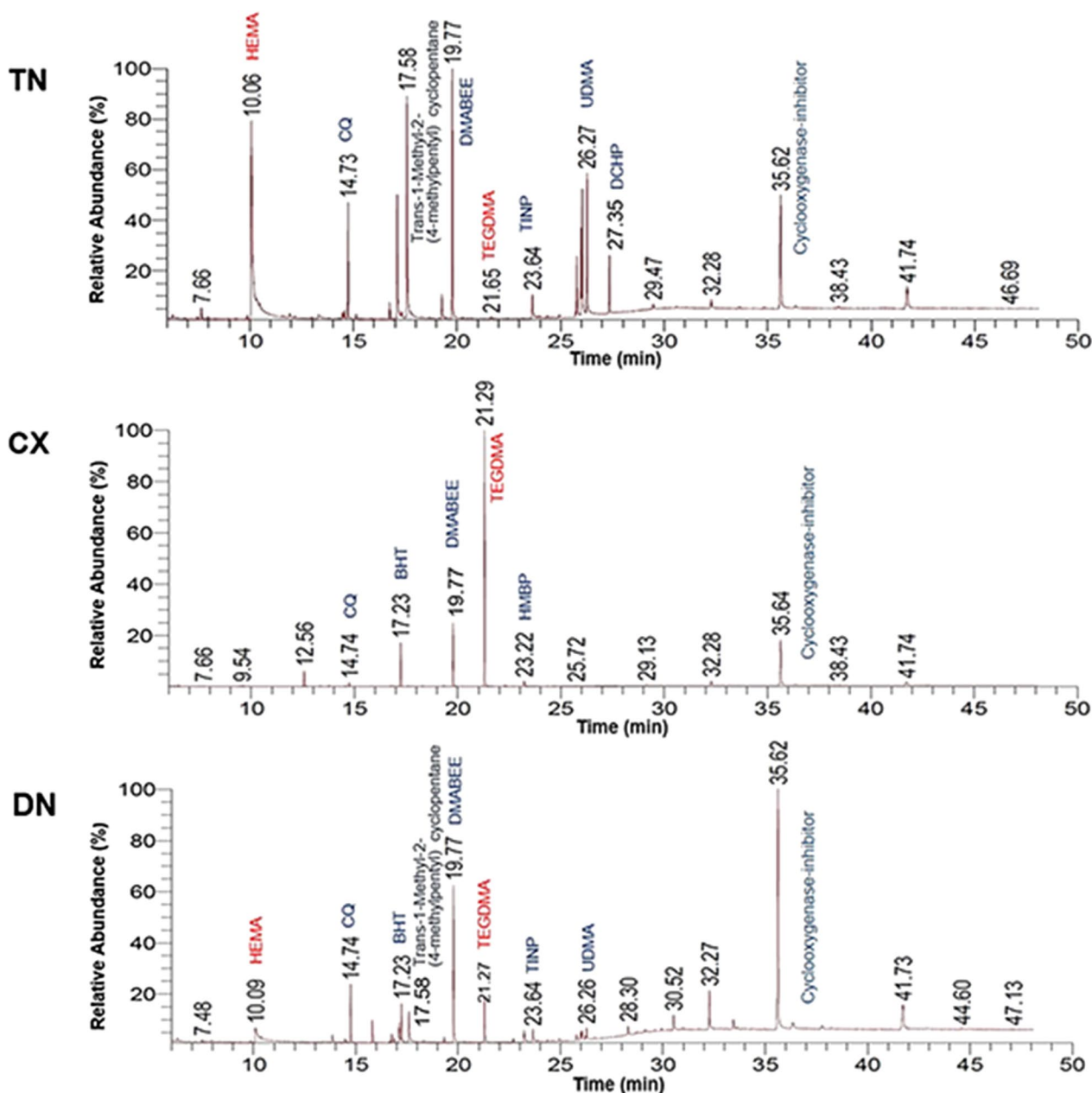


**Fig. 5** GC/MS chromatogram of the qualitative analysis. Differences in components and relative abundance of monomers and additives in TN, CX, and DN were confirmed

GC/MS experimental method is based on the vaporization and ionization of ingredients of low molecular weight compounds. And methanol was chosen to meet the limit of quantified detection due to its major dissolution efficiency. In the results, CX showed the highest TEGDMA level and had the lowest cell viability, as well as a time-dependent increase in ROS production.

As for HEMA, the value detected in TN (1.9 mM) was higher than in DN (0.34 mM) and CX (non-detect). It was widely reported that HEMA could be a degradation product from UDMA as being a basic monomer with high molecular weight [35]. UDMA is also a basic component in the TN, as claimed by the manufacturer, and the higher concentration of HEMA detected in TN was



**Table 3** Qualitative analysis by GC/MS

Compound name	Function	Formula	Molecular weight	$t_r$ (min)	Area%		
					TN	CX	DN
2-Hydroxyethyl methacrylate (HEMA)	Monomer	C <sub>6</sub> H <sub>10</sub> O <sub>3</sub>	130.14	10.06	21.70 ± 0.30	–	4.46 ± 0.15
Triethylene glycol dimethacrylate (TEGDMA)	Monomer	C <sub>14</sub> H <sub>22</sub> O <sub>6</sub>	286.32	21.65	0.26 ± 0.10	48.87 ± 3.90	3.77 ± 0.39
Camphorquinone (CQ)	Photoinitiator	C <sub>10</sub> H <sub>14</sub> O <sub>2</sub>	166.22	14.73	4.36 ± 0.58	0.78 ± 0.12	4.47 ± 0.18
4-Dimethyl amino benzoic acid ethyl ester (DMABEE)	Co-initiator	C <sub>11</sub> H <sub>15</sub> NO <sub>2</sub>	193.24	19.77	9.02 ± 1.65	12.93 ± 1.85	13.49 ± 0.21
Benzyl iodide	Others	C <sub>7</sub> H <sub>7</sub> I	218.03	12.55	–	3.81 ± 0.77	–
Butylated hydroxytoluene (BHT)	Inhibitor	C <sub>15</sub> H <sub>24</sub> O	220.35	17.23	–	8.82 ± 2.64	3.69 ± 1.61
Trans-1-methyl-2-(4-methylpentyl) cyclopentane	Others	C <sub>12</sub> H <sub>24</sub>	168.32	17.58	11.68 ± 0.27	–	4.14 ± 0.31
2-Hydroxy-4-methoxybenzophenone (HMBP)	UV-absorber	C <sub>14</sub> H <sub>12</sub> O <sub>3</sub>	228.24	23.22	–	2.02 ± 0.39	–
2-(2-Hydroxy-5-methylphenyl) benzotriazole (TINP)	UV-stabilizer	C <sub>13</sub> H <sub>11</sub> N <sub>3</sub> O	225.25	23.64	1.71 ± 0.21	–	1.49 ± 0.11
2-(3'-Hydroxy-4'-methoxyphenyl)-5-methoxy-3-(3',4',5-trimethoxyphenyl) benzofuran-6-o	Cyclooxygenase-inhibitor	C <sub>25</sub> H <sub>24</sub> O <sub>8</sub>	452.45	35.62	10.35 ± 1.55	15.85 ± 1.39	33.59 ± 1.08
4,4'-[5-(1,1-Dimethylethyl)-2-methoxy-1,3-phenylene] bisdibenzofuran	Others	C <sub>35</sub> H <sub>28</sub> O <sub>3</sub>	496.59	41.74	3.61 ± 0.90	1.67 ± 0.15	5.89 ± 0.07
Dicyclohexyl phthalate (DCHP)	Plasticizer	C <sub>20</sub> H <sub>26</sub> O <sub>4</sub>	330.42	27.35	2.46 ± 0.18	–	–

regarded to be derived from UDMA. In our GC/MS, a standard UDMA ( $\geq 97\%$ , Sigma-Aldrich, Cat no. 72869–86-4) was analysed, and the peaks were confirmed as four single peaks and one single peak of HEMA (Fig. 6B). In a previous study involving monomer releases from dentin bonding systems, when using methanol to extract the resin components, the mean content of HEMA in methanol was 10 times higher than that in distilled water [36]. Upon oxidation, the cell ROX green reagent binds to DNA and thus, its signal is primarily localised in the nucleus and mitochondria. The EC<sub>50</sub> values of HEMA for the viability of HGFs were 11.2 mM and the concentration inducing DNA strand breakdown was 1.12 mM [14]. Despite being overly extracted in methanol, HEMA was prominently detected in the TN group and might have an impact on the generation of ROS. Conventionally, BPA is a component that has been at the centre of debates due to its xeno-estrogenic potential, resulting in systemic consequences. However, many previous studies that applied highly sensitive analytical methods did not reveal the presence of BPA, despite the possible presence as an impurity during manufacturing. Biodegradation of BPA-based basic monomers into BPA was also feasible under the extremes of the oral environment such as pH fluctuation, enzymatic degradation, and thermal and mechanical challenges. Still, only trace amounts could be detected under hazardous limits, particularly with

the experimental settings for short-term elution [18]. Even with methanol as an immersion medium to dissolve extractable compounds, we did not detect BPA in the eluates from the three composites.

In our study, the level of DC reached around 70% without significant differences among the composite. Therefore, the differences in the releases of unpolymerised monomers seemed not to result from different degrees of polymerisation of composites. It was interesting that no significant cytotoxicity or ROS generation was revealed in the DN group. Apart from the relatively low elution of TEGDMA and HEMA in DN, the volumetric content of fillers is higher in DN than in others (Table 1). We assumed that the lower content of matrix monomer in DN might contribute to the smaller amount of monomer release, resulting in better biocompatibility. Another point to consider for the relatively lower level of cytotoxicity detected in DN is that DN does not contain any fluoride compounds that are claimed to be the contents of TN and CX. Previous studies showed that even novel composites containing synthetic fillers conjugated with fluoride ions revealed significant levels of anti-cariogenic potential, but not any detectable level of cytotoxicity [37, 38]. However, it will be meaningful to investigate the ionic release capacity of the composites aside from their monomer elution.

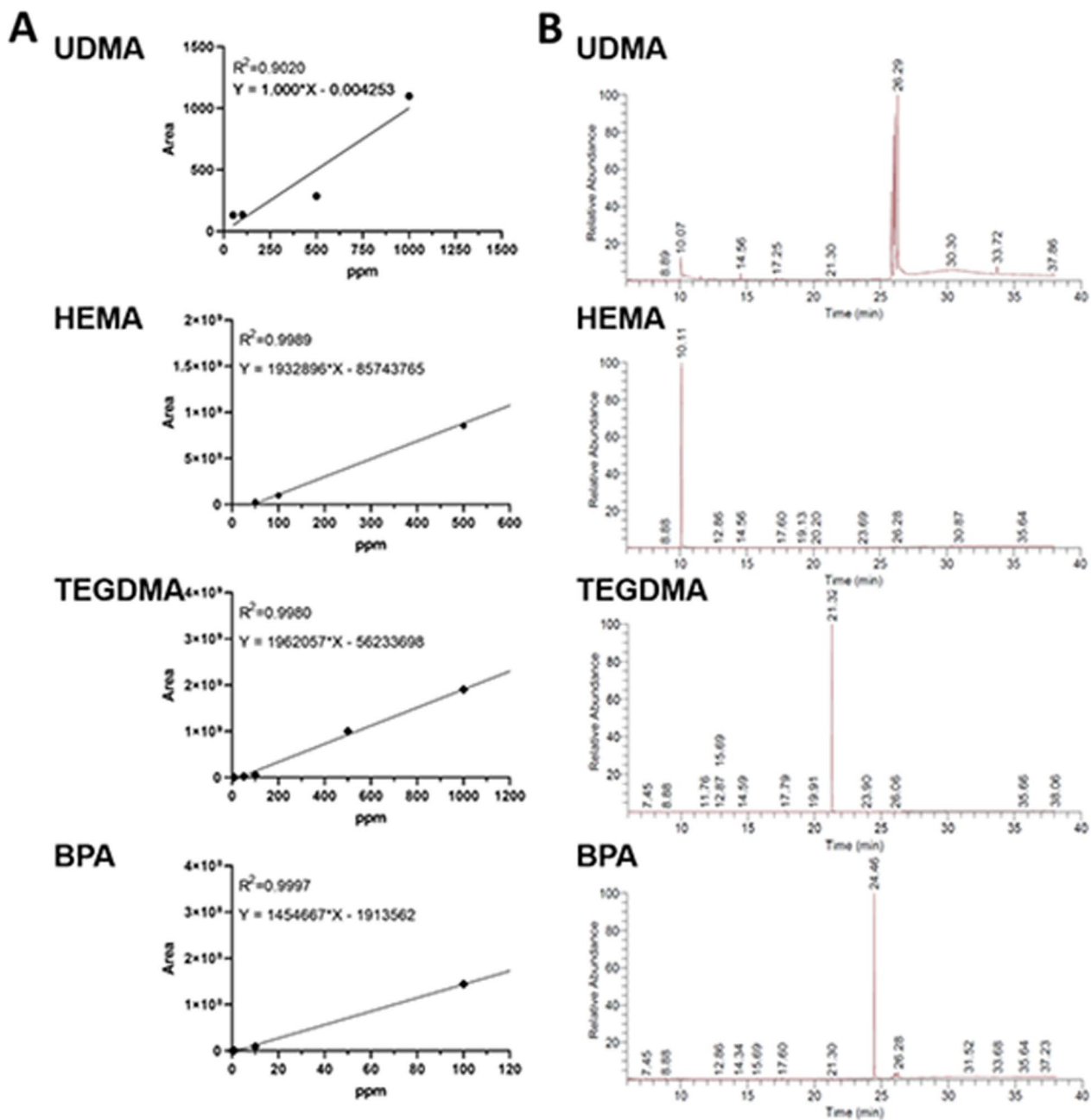


**Fig. 6** Calibration of selected standard components (UDMA, HEMA, TEGDMA, and BPA). **A** Calibration curves. The equations were used for the quantitative analysis. **B** Relative abundance of the standard components

**Table 4** Quantitative analysis of HEMA, TEGDMA, and BPA. Data are presented as the mean and standard deviation in  $\mu\text{g/mL}$  (mM)

	HEMA	TEGDMA	BPA
TN	259.46 $\pm$ 53.14 <sup>a</sup> (1.99 $\pm$ 0.41)	23.3 $\pm$ 0.06 <sup>a</sup> (0.08 $\pm$ 0.00)	Not detected
CX	Not detected	1081.10 $\pm$ 128.60 <sup>b</sup> (3.77 $\pm$ 0.45)	Not detected
DN	43.91 $\pm$ 3.32 <sup>b</sup> (0.34 $\pm$ 0.02)	38.80 $\pm$ 3.50 <sup>a</sup> (0.13 $\pm$ 0.12)	Not detected
<i>p</i>	0.0022*	< 0.0001	–

\* Result of the unpaired *t*-test between TN and DN

Different superscripts indicate significant differences in a column (*p* < 0.05)

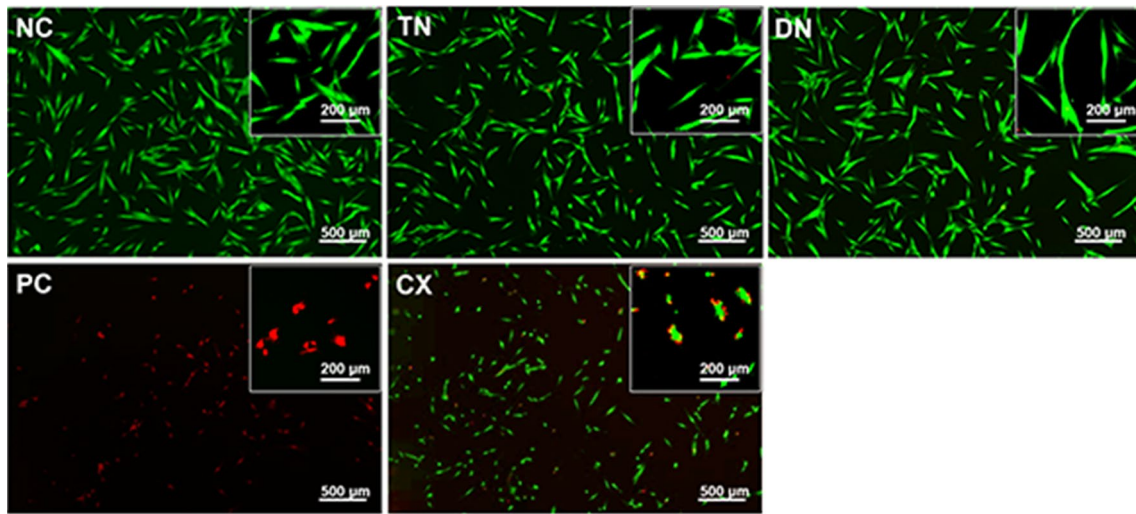


**Fig. 7** Representative images of live/dead assay. The merged fluorescent images with viable cells appear in green and dead cells in red. Dead cells and shrinkage of the cells were apparent in CX compared with NC, TN, and DN. TN and DN showed a slight decrease in cell density compared to NC

Regarding our limited experimental designs, it is hard to extrapolate the results to clinical circumstances. Since restorative composite resins are composed of various compounds, no single detection method can achieve the evaluation of every compound with various molecular weights and chemical formulas. We will need extended chemical analysis to evaluate monomers of higher

molecular weights such as Bis-GMA and UDMA [39]. The selection of the immersion medium is a complicated issue. Even when human saliva is used, the thermal, chemical, and bacterial conditions need to be incorporated to assimilate in vivo circumstances [40]. To simulate salivary flushing in the mouth, constant exchange of immersion medium also needs to be considered. In addition, mechanical impacts on restorative surfaces during intraoral service of dental composites should be considered, since dislodgement of surface fillers from the matrix can be developed, accelerating monomer elution [41]. Future studies need to investigate more clinically relevant conditions and reflect those factors in experimental settings.

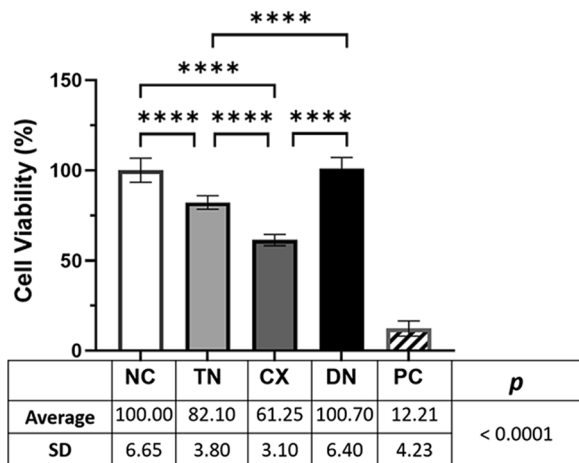


**Fig. 8** Relative cell viability by WST-1 assay. TN and CX showed significantly decreased cell viability compared with NC and DN (\*\*\*\**p* < 0.0001). NC and DN showed no significant difference after 24 h

### Conclusion

Based on this in vitro study, three nanohybrid dental composites exhibited various compositions of filler sizes and resin components, resulting in different levels of cytotoxicity and ROS production. Chemical compositions of dental composites can be considered with their biological impact on safety issues in the intraoral use of dental restorative composites. The composite eluate (CX) with the highest TEGDMA showed the highest cytotoxicity induced by ROS accumulation. The composites eluate (DN) with the lower TEGDMA and HEMA presented the highest cell viability.

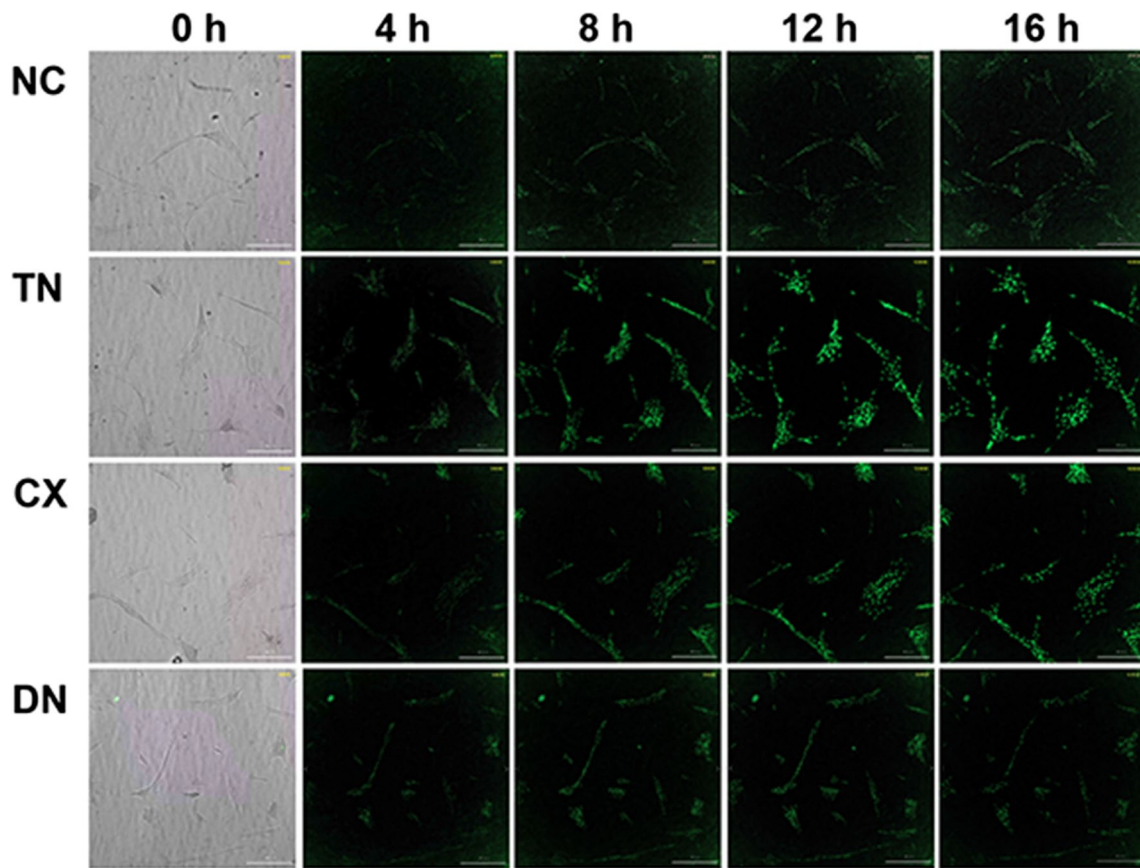


**Fig. 9** Representative images of real-time ROS (4 ×). The fluorescence intensity was observed for 16 h after the treatment with composite eluates. The green fluorescence was more evident in TN and CX compared to NC

**Table 5** GFP expression intensities in mean ± standard deviation

	0 h	4 h	8 h	12 h	16 h
NC	2712 ± 74 <sup>a</sup>	2632 ± 70 <sup>a</sup>	2687 ± 26 <sup>a</sup>	2805 ± 82 <sup>a</sup>	2946 ± 180 <sup>a</sup>
TN	2633 ± 219 <sup>a</sup>	2567 ± 145 <sup>a</sup>	3080 ± 61 <sup>b</sup>	3723 ± 119 <sup>b</sup>	3825 ± 120 <sup>b</sup>
CX	2618 ± 59 <sup>a</sup>	2554 ± 41 <sup>a</sup>	2851 ± 34 <sup>c</sup>	3132 ± 104 <sup>c</sup>	3526 ± 158 <sup>c</sup>
DN	2663 ± 46 <sup>a</sup>	2585 ± 28 <sup>a</sup>	2727 ± 93 <sup>a</sup>	2853 ± 93 <sup>a</sup>	2962 ± 50 <sup>a</sup>
<i>p</i>	0.3846	0.2395	< 0.0001	< 0.0001	< 0.0001

Different superscripts indicate significant differences in a column (*p* < 0.05)

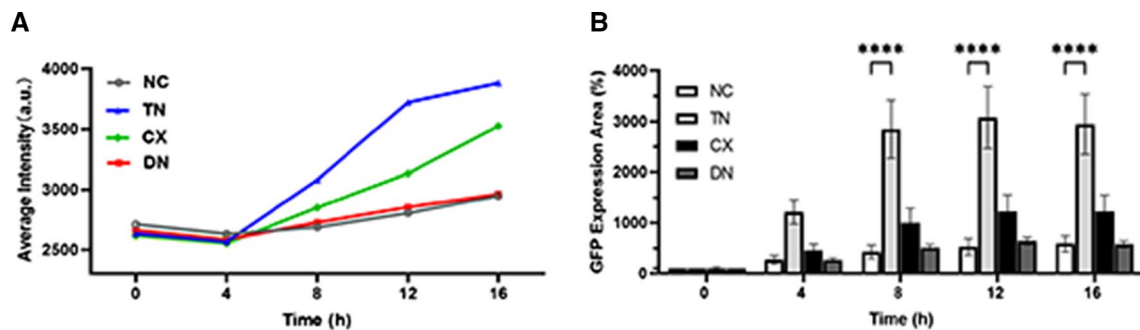


**Fig. 10** Fluorescence intensity and expression area of GFP. **A** Relative intensities of green fluorescence at each time interval. After 8 h, significantly higher intensities were detected in TN and CX compared to NC. **B** Relative GFP expression areas were calculated using relative values at zero hours. TN showed significant increases at 8 h, 12 h, and 16 h compared to NC. (\*\*\*\**p* < 0.0001)

**Table 6** Relative GFP expression area in mean ± standard deviation (%)

	0 h	4 h	8 h	12 h	16 h
NC	100.00 ± 0.00 <sup>a</sup>	273.36 ± 253.63 <sup>a</sup>	428.27 ± 401.26 <sup>a</sup>	527.69 ± 484.40 <sup>a</sup>	587.12 ± 480.53 <sup>a</sup>
TN	100.00 ± 0.00 <sup>a</sup>	1214.73 ± 723.05 <sup>a</sup>	2848.86 ± 1721.45 <sup>b</sup>	3075.96 ± 1836.66 <sup>b</sup>	2945.94 ± 1779.69 <sup>b</sup>
CX	100.00 ± 0.00 <sup>a</sup>	465.22 ± 355.18 <sup>a</sup>	1005.96 ± 844.07 <sup>a</sup>	1229.27 ± 978.90 <sup>a</sup>	1227.90 ± 958.57 <sup>a</sup>
DN	100.00 ± 0.00 <sup>a</sup>	271.90 ± 113.32 <sup>a</sup>	516.21 ± 174.13 <sup>a</sup>	642.89 ± 229.58 <sup>a</sup>	577.71 ± 192.06 <sup>a</sup>
<i>p</i>	> 0.0999	> 0.0999	< 0.0001	< 0.0001	< 0.0001

Different superscripts indicate significant differences in a column (*p* < 0.05)

**Abbreviations**

ROS	Reactive oxygen species
MAPK	Mitogen-activated protein kinase
DC	Degree of conversion
Area%	Peak area in percentage
HEMA	2-Hydroxyethyl methacrylate
TEGDMA	Triethylene glycol dimethacrylate
CQ	Camphorquinone
DMABEE	4-Dimethyl amino benzoic acid ethyl ester
BHT	Butylated hydroxytoluene
HMBP	2-Hydroxy-4-methoxybenzophenone
TINP	2-(2-Hydroxy-5-methyl phenyl) benzotriazole
DCHP	Dicyclohexyl phthakate

**Supplementary Information**

The online version contains supplementary material available at <https://doi.org/10.1186/s12903-023-02710-y>.

**Additional file 1: video S1** Real-time ROS detection in HGF-1. Nano-hybrid composites eluate results in a time-dependent increase in ROS production in HGF-1.

**Acknowledgements**

Not applicable.

**Author contributions**

E.-S. J., J.C.: wrote the main manuscript text, prepared and interpreted data. S.H.C., E.-S. J.: study concept and design. E.-S. J.: performed experiments, analysed data. B.-S.L., J.C., and S.H.C.: reviewed and edited manuscript text. W.M. and B.-S.L.: investigated and validated. S.H.C.: acquired the funding and managed the project. All authors have read and approved the final manuscript.

**Funding**

This work was supported by the Korea Medical Device Development Fund grant funded by the Korea government (the Ministry of Science and ICT, the Ministry of Trade, Industry and Energy, the Ministry of Health & Welfare, the Ministry of Food and Drug Safety) (Project Number: 9991006717, KMDF\_PR\_20200901\_0044).

**Availability of data and materials**

The data and materials used and/or analysed during the current study are available from the corresponding author upon reasonable request.

**Declarations**

**Ethics approval and consent to participate**

Not applicable.

**Consent for publication**

Not applicable.

**Competing interests**

The authors declare that they have no conflict of interest.

**Author details**

<sup>1</sup>Department of Dental Biomaterials Science, School of Dentistry and Dental Research Institute, Seoul National University, 101 Daehak-Ro, Jongno-Gu, Seoul 03080, Republic of Korea. <sup>2</sup>Department of Stomatology, Yanbian University and Affiliated Hospital of Yanbian University, Yanji 133000, China. <sup>3</sup>Harvard Medical School, Boston, MA 02115, USA. <sup>4</sup>Wellman Center for Photomedicine, Massachusetts General Hospital, Boston, MA 02114, USA. <sup>5</sup>National Dental Care Center for Persons With Special Needs, Seoul National University Dental Hospital, 101 Daehak-Ro, Jongno-Gu, Seoul 03080, Republic of Korea.

Received: 7 July 2022 Accepted: 3 January 2023

Published online: 30 January 2023

**References**

1. Van Dijken J, Pallesen U. A randomized 10-year prospective follow-up of class II nanohybrid and conventional hybrid resin composite restorations. *J Adhes Dent.* 2014;16:585–92.
2. Alzraikat H, Burrow M, Maghaireh G, Taha N. Nanofilled resin composite properties and clinical performance: a review. *Oper Dent.* 2018;43:E173–90.
3. Durner J, Obermaier J, Draenert M, Ilie N. Correlation of the degree of conversion with the amount of elutable substances in nano-hybrid dental composites. *Dent Mater.* 2012;28:1146–53.
4. Yadav R, Meena A, Patnaik A. Biomaterials for dental composite applications: a comprehensive review of physical, chemical, mechanical, thermal, tribological, and biological properties. *Polym Adv Technol.* 2022;33:1762–81.
5. Bastos NA, Bitencourt SB, Martins EA, De Souza GM. Review of nanotechnology applications in resin-based restorative materials. *J Esthet Dent.* 2021;33:567–82.
6. Heintze S, Forjanic M, Ohmiti K, Rousson V. Surface deterioration of dental materials after simulated toothbrushing in relation to brushing time and load. *Dent Mater.* 2010;26:306–19.
7. Kaizer MR, de Oliveira-Ogliari A, Cenci MS, Opdam NJ, Moraes RR. Do nanofill or submicron composites show improved smoothness and gloss? A systematic review of in vitro studies. *Dent Mater.* 2014;30:e41–78.
8. Maran BM, de Geus JL, Gutiérrez MF, Heintze S, Tardem C, Barceleiro MO, Reis A, Loguercio AD. Nanofilled/nanohybrid and hybrid resin-based composite in patients with direct restorations in posterior teeth: A systematic review and meta-analysis. *J Dent.* 2020;99: 103407.
9. Nasution H, Tantra A, Arista T. The effect of filler content and particle size on the impact strength and water absorption of epoxy/cockle-shell powder (*Anadora granosa*) composite. *ARPN J Eng Appl Sci.* 2016;11:4739–42.
10. Örtengren U, Wellendorf H, Karlsson S, Ruyter I. Water sorption and solubility of dental composites and identification of monomers released in an aqueous environment. *J Oral Rehabil.* 2001;28:1106–15.
11. Van Landuyt K, Nawrot T, Geebelen B, De Munck J, Snauwaert J, Yoshihara K, Scheers H, Godderis L, Hoet P, Van Meerbeek B. How much do

- resin-based dental materials release? A Meta-Anal Approach Dent Mater. 2011;27:723–47.
12. Bationo R, Rouamba A, Diarra A, Beugré-Kouassi MLA, Beugré JB, Jordana F. Cytotoxicity evaluation of dental and orthodontic light-cured composite resins. *Clin Exp Dent Res*. 2021;7:40–8.
  13. Yang Y, Reichl FX, Shi J, He X, Hickel R, Högg C. Cytotoxicity and DNA double-strand breaks in human gingival fibroblasts exposed to eluates of dental composites. *Dent Mater*. 2018;34:201–8.
  14. Urcan E, Scherthan H, Styllou M, Haertel U, Hickel R, Reichl FX. Induction of DNA double-strand breaks in primary gingival fibroblasts by exposure to dental resin composites. *Biomaterials*. 2010;31:2010–4.
  15. Schmalz G. Determination of biocompatibility: evaluation of materials. In: Schmalz G, Arenholt D, editors. *Biocompatibility of dental materials*. Leipzig: Springer; 2009. p. 13–43.
  16. Peskersoy C, Oğuzhan A, Gurlek O. The effect of flowable composite resins on periodontal health, cytokine levels, and immunoglobulins. *Biomed Res Int*. 2022;23(2022):6476597. <https://doi.org/10.1155/2022/6476597>.
  17. Lee DH, Kim NR, Lim B-S, Lee Y-K, Yang H-C. Effects of TEGDMA and HEMA on the expression of COX-2 and iNOS in cultured murine macrophage cells. *Dent Mater*. 2009;25:240–6.
  18. De Nys S, Duca RC, Vervliet P, Covaci A, Boonen I, Elskens M, Vanoirbeek J, Godderis L, Van Meerbeek B, Van Landuyt KL. Bisphenol A as degradation product of monomers used in resin-based dental materials. *Dent Mater*. 2021;37:1020–9.
  19. Volk J, Engelmann J, Leyhausen G, Geurtsen W. Effects of three resin monomers on the cellular glutathione concentration of cultured human gingival fibroblasts. *Dent Mater*. 2006;22:499–505.
  20. Eckhardt A, Gerstmayr N, Hiller KA, Bolay C, Spagnuolo G, Camargo C, Schmalz G, Schweikl H. TEGDMA-induced oxidative DNA damage and activation of ATM and MAP kinases. *Biomaterials*. 2009;30:2006–14.
  21. Nocca G, De Palma F, Minucci A, De Sole P, Martorana GE, Callà C, Morlacchi C, Gozzo ML, Gambarini G, Chimenti C. Alterations of energy metabolism and glutathione levels of HL-60 cells induced by methacrylates present in composite resins. *J Dent*. 2007;35:187–94.
  22. Schweikl H, Spagnuolo G, Schmalz G. Genetic and cellular toxicology of dental resin monomers. *J Dent Res*. 2006;85:870–7.
  23. Shehata M, Durner J, Eldenez A, Van Landuyt K, Styllou P, Rothmund L, Hickel R, Scherthan H, Geurtsen W, Kaina B. Cytotoxicity and induction of DNA double-strand breaks by components leached from dental composites in primary human gingival fibroblasts. *Dent Mater*. 2013;29:971–9.
  24. Koulaouzidou EA, Roussou K, Sidiropoulos K, Nikolaidis A, Kolokuris I, Tsakalof A, Tsitsimpikou C, Kouretas D. Investigation of the chemical profile and cytotoxicity evaluation of organic components eluted from pit and fissure sealants. *Food Chem Toxicol*. 2018;120:536–43.
  25. Susila AV, Balasubramanian V. Correlation of elution and sensitivity of cell lines to dental composites. *Dent Mater*. 2016;32:e63–72.
  26. Krifka S, Seidenader C, Hiller KA, Schmalz G, Schweikl H. Oxidative stress and cytotoxicity generated by dental composites in human pulp cells. *Clin Oral Investig*. 2012;16:215–24.
  27. Kashiwagi K, Inoue H, Komasa R, Hosoyama Y, Yamashita K, Morisaki A, Goda S. Optimal dilutions of S-PRG filler eluate for experiments on human gingival fibroblasts in vitro. *Dent Mater J*. 2021;40:136–42.
  28. Reidelbach C, Garcia-Käufer M, Wingert N, Arif A, Vach K, Hellwig E, Gminski R, Polydorou O. Cytotoxicity and estrogenicity in simulated dental wastewater after grinding of resin-based materials. *Dent Mater*. 2021;37:1486–97.
  29. De Angelis F, Sarteur N, Buonvivere M, Vadini M, Šteffl M, D'Arcangelo C. Meta-analytical analysis on components released from resin-based dental materials. *Clin Oral Investig*. 2022. <https://doi.org/10.1007/s00784-022-04625-4>.
  30. Spahl W, Budzikiewicz H, Geurtsen W. Determination of leachable components from four commercial dental composites by gas and liquid chromatography/mass spectrometry. *J Dent*. 1998;26:137–45.
  31. Di Franciscantonio M, Pacheco RR, Aguiar TR, Boaro LCC, Braga RR, Martins AL, Giannini M. Evaluation of composition and morphology of filler particles in low-shrinkage and conventional composite resins carried out by means of SEM and EDX. *J Clin Dent Res*. 2016;13:49–58.
  32. Delvallée A, Feltin N, Ducourtieux S, Trabelsi M. Comparison of nanoparticle diameter measurements by atomic force microscopy and scanning electron microscopy. In: 16th international congress of metrology. EDP Sciences. 2013. [https://cfmetrology.edpsciences.org/articles/metrology/abs/2013/01/metrology\\_metr2013\\_06007/metrology\\_metr2013\\_06007.html](https://cfmetrology.edpsciences.org/articles/metrology/abs/2013/01/metrology_metr2013_06007/metrology_metr2013_06007.html) Accessed: 27 Sep 2022.
  33. Cebe MA, Cebe F, Cengiz MF, Cetin AR, Arpag OF, Ozturk B. Elution of monomer from different bulk fill dental composite resins. *Dent Mater*. 2015;31:e141–9.
  34. Reichl FX, Seiss M, Marquardt W, Kleinsasser N, Schweikl H, Kehe K, Hickel R. Toxicity potentiation by H<sub>2</sub>O<sub>2</sub> with components of dental restorative materials on human oral cells. *Arch Toxicol*. 2008;82:21–8.
  35. Michelsen VB, Moe G, Skålevik R, Jensen E, Lygre H. Quantification of organic eluates from polymerized resin-based dental restorative materials by use of GC/MS. *J Chromatogr B*. 2007;850:83–91.
  36. Reichl FX, Löhle J, Seiss M, Furche S, Shehata MM, Hickel R, Müller M, Dränert M, Durner J. Elution of TEGDMA and HEMA from polymerized resin-based bonding systems. *Dent Mater*. 2012;28:1120–5.
  37. Wei SuL, Lin DJ, Yen UJ. Novel dental resin composites containing LiAl-F layered double hydroxide (LDH) filler: fluoride release/recharge, mechanical properties, color change, and cytotoxicity. *Dent Mater*. 2019;35:663–72.
  38. Zheng L, Li K, Ning C, Sun J. Study on antibacterial and fluoride-releasing properties of a novel composite resin with fluorine-doped nano-zirconia fillers. *J Dent*. 2021;113: 103772.
  39. Putzeys E, Cokic SM, Chong H, Smet M, Vanoirbeek J, Godderis L, et al. Simultaneous analysis of bisphenol A based compounds and other monomers leaching from resin-based dental materials by UHPLC–MS/MS. *J Sep Sci*. 2017;40:1063–75.
  40. Boaro LC, Lopes DP, de Souza AS, Nakano EL, Perez MD, Pfeifer CS, et al. Clinical performance and chemical-physical properties of bulk fill composites resin—a systematic review and meta-analysis. *Dent Mater*. 2019;35:e249–64.
  41. Rinastiti M, Özcan M, Siswomihardjo W, Busscher HJ. Effects of surface conditioning on repair bond strengths of non-aged and aged micro-hybrid, nanohybrid, and nanofilled composite resins. *Clin Oral Investig*. 2011;15:625–33.

## Publisher's Note

Springer Nature remains neutral with regard to jurisdictional claims in published maps and institutional affiliations.

Ready to submit your research? Choose BMC and benefit from:

- fast, convenient online submission
- thorough peer review by experienced researchers in your field
- rapid publication on acceptance
- support for research data, including large and complex data types
- gold Open Access which fosters wider collaboration and increased citations
- maximum visibility for your research: over 100M website views per year

At BMC, research is always in progress.

Learn more [biomedcentral.com/submissions](https://biomedcentral.com/submissions)

